Anomalous Inelastic Neutron Scattering in bcc Zr-Nb Alloys*

J. D. Axe and D. T. Keating†
Brookhaven National Laboratory, Upton, New York 11973

and

S. C. Moss‡
Department of Physics, University of Houston, Houston, Texas 77004

(Received 21 April 1975)

Inelastic neutron scattering from bcc $Zr_{0.92}Nb_{0.08}$ at 965°C reveals features in the inelastic response which lack the average cubic symmetry of the lattice. This can be understood as arising from phonon modulation of quasistatic short-range order representing fluctuations into an incipient "ω" phase.

At high temperatures the binary alloy $Zr_{1-x}Nb_x$ ($0<x<0.2$) forms a random bcc phase, which at lower temperatures transforms into a metastable "ω" phase,[1,2] related to the parent bcc phase by the condensation of static longitudinal plane-wave atomic displacements along [111] with a wave vector $\vec{\kappa}_\omega=\frac{2}{3}\langle 111\rangle$ (which can be equivalently described as a transverse wave with $\vec{\kappa}_\omega=\frac{1}{3}\times\langle 112\rangle$).[3] The favorable Coulombic energy associated with this mode of distortion[4] results in a minimum in the appropriate phonon dispersion near this wave vector for most bcc metals, suggesting a soft-mode mechanism, although the bcc-ω transformation is of necessity first order.[5] A previous neutron-scattering study of bcc $Zr_{0.8}Nb_{0.2}$ looking for such effects succeeded mainly in showing that short-wavelength phonon groups were surprisingly poorly defined, and also documented the existence of strong quasistatic ω-like short-range order well into the bcc-phase field.[6] This Letter reports further measurements on a more dilute alloy $Zr_{0.92}Nb_{0.08}$ at $T=965$°C. Although this temperature is well within the bcc single-phase field, the inelastic scattering function $S(\vec{Q},\omega)$ is shown to have anomalous structure which violates the expected cubic symmetry and which can be related to these persistent ω fluctuations in the bcc phase.

The essential features of our observations are summarized in Fig. 1 which shows the results of the triple-axis spectrometer scans in a scattering geometry designed to measure phonons with q along [112] and displacements along [111] about the [222] bcc reciprocal-lattice point. Cubic symmetry requires that scans A and B towards opposite Brillouin-zone boundaries (ZB) be identical, but the actual data shown in Fig. 2 reveal that this is not the case.[7] The shaded area in Fig. 1 is a measure of the uncertainty of the phonon "branches" of Fig. 2 and is necessarily somewhat arbitrary particularly near the ZB on branch B. Note that this transverse ZB phonon would be the soft mode were this description to be appropriate. A closely related remark is that the long-lived ω-like fluctuations show up as quasielastic diffuse scattering around these same ZB wave vectors, accounting for the elastic central peaks seen in Fig. 2. The fact that this diffuse elastic scattering itself lacks cubic symmetry (much as in Ref. 6) suggests where to look for similar asymmetries in the inelastic scattering.

In fact, while these inelastic-scattering results are clearly inconsistent with what is expected for

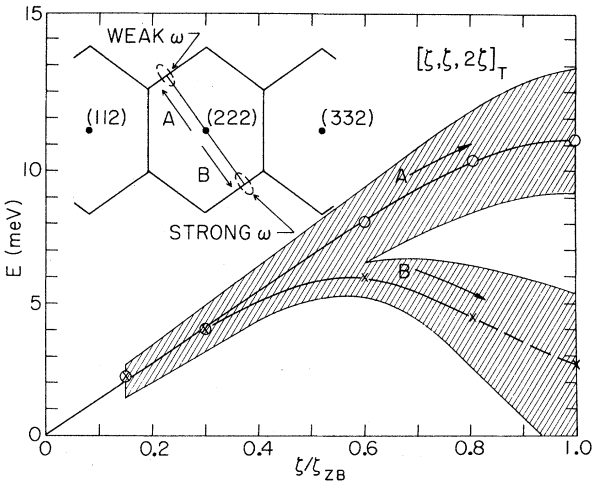

FIG. 1. A summary of phonon branches obtained from an analysis of data shown in Fig. 2. The inset shows the positions in reciprocal space at which the data were taken. The dashed ellipses indicating diffuse elastic scattering, denoted by weak ω and strong ω, are centered on the zone-boundary points given by the set $\frac{1}{3}[112]$. These become the ω-phase Bragg peaks at low temperature as do all the ZB members of the set. Cubic symmetry requires scans A and B to be identical.

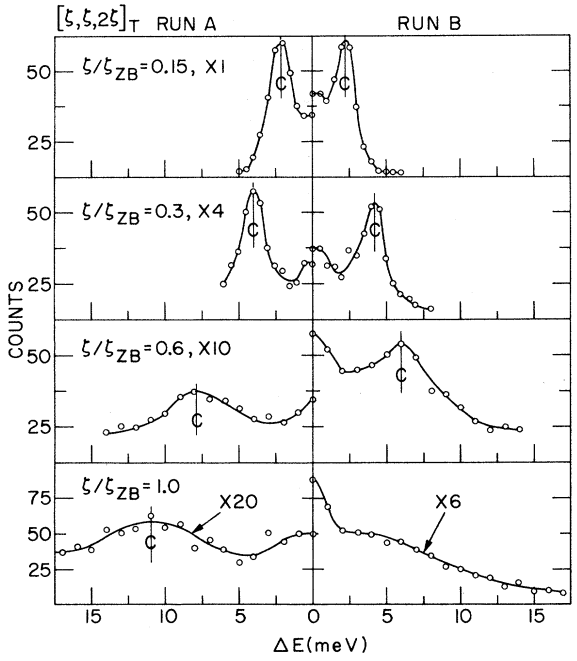

FIG. 2. Inelastic scattering spectra for bcc $Zr_{0.92}$-$Nb_{0.08}$ at 965°C. The two halves of the figure refer not to energy loss and energy gain but to different symmetric locations in reciprocal space. (See Fig. 1.)

a simple monatomic bcc lattice, the principle features can be understood by considering the influence of the static ω-like short-range order on the inelastic scattering. We express the instantaneous position of the atom within the Lth bcc unit cell as

$$\vec{r}_L(t) = \vec{R}_L + \sum_\lambda P_{L\lambda}\vec{\xi}_\lambda + \vec{\mu}_L(t),$$

where $\vec{\mu}_L(t)$ describes the vibrational motion and $\vec{\xi}_\lambda$ are the displacements the atoms must undergo to be carried into one of the possible ω configurations. $P_{L\lambda}=1$ if the Lth atom is in the λth such configuration and is zero otherwise. The elastic scattering is composed of two terms,

$$S_{el}(\vec{Q}) = S_{bcc}(\vec{Q}) + S_{diff}(\vec{Q}),$$

where

$$S_{diff}(\vec{Q}) = \sum_{\substack{\lambda\lambda' \\ \kappa\tau}} f_\lambda(\vec{Q}) f_{\lambda'}{}^*(\vec{Q}) G_{\lambda\lambda'}(\vec{\kappa})\delta(\vec{Q}+\vec{\kappa}-\vec{\tau}). \quad (1)$$

$G_{\lambda\lambda'}(\vec{\kappa})$ is the disorder correlation function,

$$G_{\lambda\lambda'}(\vec{\kappa}) = \langle P_\lambda(\vec{\kappa}) P_{\lambda'}{}^*(\vec{\kappa})\rangle - \langle P_\lambda(0)\rangle\langle P_{\lambda'}(0)\rangle\delta(\kappa).$$

$P_\lambda(\vec{\kappa})$ is the Fourier transform of the site-occupation operator $P_{L\lambda}$, $\vec{\tau}$ is a reciprocal-lattice vector, $\langle\ \rangle$ indicates an ensemble average, and $f_\lambda(\vec{Q}) = \exp[i\vec{Q}\cdot\vec{\xi}_{\lambda e} - W(\vec{Q})]$, where $W(\vec{Q})$ is a Debye-Waller factor. $S_{bcc}(\vec{Q})$ represents the sharp Bragg scattering from the average structure and is given by replacing $G_{\lambda\lambda'}(\vec{\kappa})$ by $\langle P_\lambda(0)\rangle \times \langle P_{\lambda'}(0)\rangle\delta(\vec{\kappa})$ in Eq. (1).

Even within the harmonic approximation there are two sorts of difficulties which arise in discussing the *inelastic* scattering from such a disordered lattice. The first is the dynamical problem of describing the elastic mismatch between distorted and undistorted regions of the lattice and the resulting scattering of the bcc phonons. The second complication is purely structural in origin. Whatever the correct description of the vibrational excitations, they are modulating a structurally disordered array of scatterers, and this too must manifest itself in the inelastic-diffraction pattern. It is conceptually possible to dissociate the dynamic and structural aspects by postulating a model disordered lattice in which the harmonic restoring forces are independent of the local equilibrium configuration. The resulting structural aspect can then be discussed rather precisely, and it is worthwhile to do so, for although it is difficult to estimate the importance of the dynamical effects that are ignored, the structural effects are surely of great importance so long as $|Q\xi| \gtrsim 1$. In fact these purely structural effects contain many of the anomalous features of our experimental observations.

With the above dynamical simplification, the displacement correlation function $\langle\vec{\mu}_L(t)\vec{\mu}_L'(0)\rangle$ is independent of the static displacements $P_{L\lambda}\vec{\xi}_\lambda$ and is equal to that of the bcc lattice. It is then not difficult to show that the harmonic one-phonon scattering also consists of two parts, $S_1(\vec{Q},\omega) = S_{bcc}(\vec{Q},\omega) + S_{diff}(\vec{Q},\omega)$, where

$$S_{diff}(\vec{Q},\omega) = \left(\frac{1+n(\omega)}{\omega}\right) \sum_{\substack{\vec{q},\vec{\kappa},\vec{\tau} \\ \lambda,\lambda',j}} f_\lambda(\vec{Q}) f_{\lambda'}(\vec{Q}) G_{\lambda\lambda'}(\vec{\kappa}) A_j(\vec{q},\omega)\delta(\vec{Q}+\vec{\kappa}-\vec{q}-\vec{\tau}), \quad (2)$$

$$A_j(\vec{q},\omega) = \frac{\hbar|\vec{Q}\cdot\vec{e}_j(\vec{q})|^2}{2NM}\delta(|\omega| - \omega_j(\vec{q})).$$

Here $n(\omega)=(e^{\beta\omega}-1)^{-1}$ and $\vec{e}_j(\vec{q})$ and $\omega_j(\vec{q})$ are the eigenvector and eigenfrequency of the $(\vec{q},j)$th normal mode of the bcc lattice. Once again $S_{\rm bcc}(\vec{Q},\omega)$ can be obtained from Eq. (2) by replacing $G_{\lambda\lambda'}(\vec{\kappa})$ by $\langle P_\lambda(0)\rangle\langle P_{\lambda'}(0)\rangle\delta(\vec{\kappa})$. Note the structure of Eq. (2) and its relation to Eq. (1). Just as it is possible to associate $S_{\rm bcc}(\vec{Q},\omega)$ with the modulation of a specific Bragg peak with wave vector $\vec{\tau}=\vec{Q}-\vec{q}$ by a single phonon of wave vector $\vec{q}$, so it is possible to associate $S_{\rm diff}(\vec{Q},\omega)$ with the modulation of the quasistatic short-range order giving rise to $S_{\rm diff}(\vec{Q}-\vec{q})$ by a range of phonons with complementary wave vectors $\vec{q}$. Since the $\omega_j(\vec{q})$ are well defined in this model, $S_{\rm bcc}(\vec{Q},\omega)$ has a sharp frequency distribution. But $S_{\rm diff}(\vec{Q},\omega)$ is broadened in frequency because it consists of a convolution over many phonons,[8] the width being of order $\Delta\omega\sim[\partial\omega(q)/\partial q]\Delta\vec{\kappa}$, where $\Delta\vec{\kappa}$ is the width of $S_{\rm diff}(\vec{Q},\omega)$ in the region about $\vec{Q}=\vec{\kappa}$.

Equation (2) has been used to calculate $S_1(Q,\omega)$ and thereby the mean frequencies and integrated inelastic-scattering intensities for the values of $\vec{Q}$ shown in Fig. 2, for a simple model of the bcc lattice with short-range ω fluctuations. Because the scattering geometry strongly favors the ω variant with displacements along $\langle 111\rangle$ (there are four variants, corresponding to the four [111] directions), for simplicity only this contribution is shown in Fig. 3. $G(\vec{\kappa})$ was assumed to have an isotropic Gaussian distribution with width $\Delta\kappa=0.27(2\pi/\alpha)$ (full width at half-maximum). In calculating $f_\lambda(\vec{Q})$ a value of $|\xi|$ was used which is approximately consistent with the distribution of diffuse *elastic* scattering at the A and B zone boundaries, which in turn is not substantially different (25% smaller) than that given by Keating and LaPlaca[9] for $Zr_{0.80}Nb_{0.20}$. bcc Nb phonon frequencies[10] scaled by the factor 0.73 were used to bring the $[112]T$ ZB phonon into agreement with our observations in the alloy.

Since $S_{\rm diff}(\vec{Q})$ is strongly localized about incipient ω-phase superlattice vectors, the structure in $S_{\rm diff}(\vec{Q},\omega)$ shown in Fig. 3 can be thought of as broadened precursors of ω-phase phonon branches obtained by folding the bcc reciprocal lattice back onto itself in the appropriate manner. The narrow black bars represent the original bcc phonons, while the remaining bars represent essentially the identical bcc phonons with the origin displaced by $\vec{\kappa}_\omega-\vec{\tau}=\pm\frac{1}{3}[11\bar{2}]$. The latter are shown as broader bars to indicate qualitatively the purely structural broadening of the inelastic scattering. Features at $\omega/\omega_{\rm ZB}>1$ result from

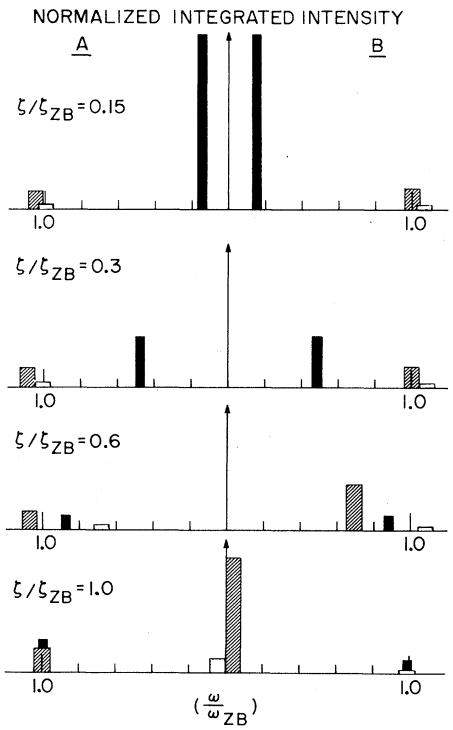

FIG. 3. Mean frequency and integrated intensities of phonon groups calculated using Eq. (2). The black bars represent a modulation of the average bcc lattice, the remainder a modulation of ω-phase short-range order.

umklapped phonons lying on the face of the bcc zone.

Figure 3 demonstrates most of the qualitative features of the experimental data of Fig. 2. At $\zeta/\zeta_{\rm ZB}=0.15$, it predicts the dominant feature to be the symmetric sharp bcc phonons, as is indeed also the case at $\zeta/\zeta_{\rm ZB}=0.30$. The experimental data did not have sufficient range to confirm the existence of the weak peaks predicted near $\omega_{\rm ZB}$. At $\zeta/\zeta_{\rm ZB}=0.60$, the bcc phonons have begun to merge with the other two branches and all we might expect experimentally is a broad response, especially if finite-lifetime effects are included. Figure 3 then suggests for scan A a broad weak peak centered on a frequency somewhat smaller than the bcc zone-boundary frequency. For scan B a broad peak of greater intensity and lower average frequency might be expected and this is observed. Finally, at the zone boundary, scan A should have a broad peak at the ZB frequency and a weak (inelastic) peak centered about zero energy transfer due to $q\simeq 0$ acoustic phonons. The relative intensities of these two features reverses for scan B with an especially dramatic increase in the *broad* inelastic scatter-

ing around $\Delta E = 0$. Figure 2 qualitatively reproduces this calculated response.

The frequencies of the calculated phonon dispersion in Fig. 3 are, as they must be, symmetrical in scans A and B, but the intensities are not. In our present interpretation the two measured "dispersion curves" shown in Fig. 1 are identical at small ζ since the bcc phonons are most strongly sampled. As ζ increases the bcc phonons broaden and merge with the excitations associated with the ω fluctuations. The average frequency of this broad band differs between scans A and B because of asymmetries in the inelastic structure factor for these ω-phase phonons.

Finally what can be said about the soft-mode hypothesis? The data summarized in Fig. 1, particularly scan B taken alone, show the behavior expected of a soft-phonon branch, with the ZB mode itself overdamped. But the present calculations show that it is reasonable to attribute this low-frequency scattering not to a genuine soft mode, i.e., an incipient lattice instability, but rather to the modulation of quasistatic short-range order by ordinary low-frequency long-wavelength sound waves. *It is clear that this effect can occur generally in other similar circumstances.* Concerning the bcc-ω phase transformation it seems that the soft-mode description is inappropriate in that the important premonitory fluctuations involved occur at much lower than phononlike frequencies and in fact appear essentially static in these experiments.

*Work performed under the auspices of the U. S. Energy Research and Development Administration.

†Present address: 1325 North Nutmeg Avenue, Escondido, Calif. 92096.

‡Guest scientist at Brookhaven National Laboratory, Upton, N. Y. 11973.

[1]B. A. Hatt and J. A. Roberts, Acta Metall. 8, 575 (1960); C. W. Dawson and S. L. Sass, Metall. Trans. 1, 2225 (1970).

[2]B. S. Hickman, J. Mater. Sci. 4, 554 (1969).

[3]D. de Fontaine, Acta Metall. 18, 275 (1970).

[4]D. L. Price, K. S. Singwi, and M. P. Tosi, Phys. Rev. B 2, 2983 (1970).

[5]H. E. Cook, Acta Metall. 21, 1445 (1973).

[6]S. C. Moss, D. T. Keating, and J. D. Axe, in *Phase Transitions—1973,* edited by L. E. Cross (Pergamon, New York, 1973), p. 179.

[7]In order to make the comparisons for comparable instrumental resolution, scan A was taken for phonon annihilation and scan B for phonon creation.

[8]Note that in the convolution, $f_\lambda(\vec{Q})$ not $f_\lambda(\vec{Q}-\vec{q})$ appears, so that the weighting of the inelastic intensity is not simply proportional to the intensity of the complementary elastic diffuse scattering, $S_{\mathrm{diff}}(\vec{Q}-\vec{q})$.

[9]D. T. Keating and S. C. LaPlaca, J. Phys. Chem. Solids 35, 879 (1974).

[10]R. I. Sharp, J. Phys. C: Solid State Phys. 2, 421 (1969). Pure bcc Zr phonons have not been measured because of difficulties associated with obtaining a single crystal. However, it is likely that the lattice dynamics of this dilute Nb alloy are very similar to bcc Zr.

Importance of Chemical Effects in Determining the Free-Electron-Like Band Structure of $K_2Pt(CN)_4Br_{0.3}\cdot 3H_2O$

R. P. Messmer and D. R. Salahub

Corporate Research and Development Center, General Electric Company, Schenectady, New York 12301

(Received 23 June 1975)

It is shown that a three-band model (i.e., inclusion of $5d_{z^2}$, $6s$, and $6p_z$ states) for the linear Pt chains in $K_2Pt(CN)_4Br_{0.3}\cdot 3H_2O$ is inappropriate for a description of the electronic structure. The chemical effects of the ligands force an s-d hybridization which is k independent and leads to free-electron-like bands within a basically tight-binding scheme. This results in an explanation of the band structure deduced experimentally. A highly simplified model is also presented to explain the partial occupancy ($\frac{5}{6}$ full) of the band.

There has been a great deal of recent interest both experimentally[1-3] and theoretically[1,2,4-6] in the properties of a group of mixed-valence platinum salts of which $K_2Pt(CN)_4Br_{0.3}\cdot 3H_2O$ (KCP) has been the most extensively studied. A large number of properties of KCP show the behavior expected on the basis of one-dimensional physical models. For example, the Peierls distortion, which occurs only in one-dimensional systems, has been observed experimentally in KCP.[7,8]